

# On Importance of Inelastic Rescatterings in Pion Double Charge Exchange on Nuclei

A.B.Kaidalov, A.P.Krutenkova

*State Research Center  
Institute of Theoretical and Experimental Physics  
Moscow, 117259, Russia*

## Abstract

Different aspects of the Gribov–Glauber approach for calculation of inclusive pion double charge exchange (DCX) on nuclei are investigated. Recently we have shown that inelastic rescatterings (IR) with two (and more) pions in the intermediate states give an important contribution to the process of DCX at energies above  $\sim 0.6$  GeV. In this paper we use the one pion exchange model to study in details amplitudes of two pion production. This allows us to verify theoretical assumptions made in the previous paper and to predict cross section for the forward inclusive pion DCX at energies  $\gtrsim 1$  GeV, where IR dominate over the conventional DCX mechanism of two sequential single charge exchanges.

PACS:

Keywords:

## 1 Introduction

The inclusive pion double charge exchange (DCX) reaction on nuclei, e.g.

$$\pi^- + A(Z, N) \rightarrow \pi^+ + X \quad (1)$$

as a two-step transition on two like nucleons (protons) is described by the diagrams of three types (Fig.1(a), (b), (c)) which correspond to the Glauber picture of elastic (a), quasielastic (b) and inelastic (c) rescatterings.

The conventional DCX mechanism of two sequential single charge exchanges (SSCX), i.e. the elastic rescattering, is found to describe [1], in general, experimental data on pion DCX at energies of the meson factories up

to 0.5  $GeV$ . It predicts [2] a strong decrease of forward angle exclusive pion DCX at incident kinetic energies  $T_0 \gtrsim 0.6 GeV$  due to the rapid energy drop of  $\pi^- \rightarrow \pi^0$  transition rate. The SSCX mechanism leads [3] to analogous behaviour of inclusive forward DCX rate too.

Inclusive reaction (1) is a unique process where, as it was shown in [4], the effect of the Glauber inelastic rescatterings (IR) becomes very important already at  $GeV$  energies. This effect can be expected from a comparison of experimental total cross sections for two competing processes,  $\pi^- p \rightarrow \pi^0 n$  and  $\pi^- p \rightarrow \pi^+ \pi^- n$  (Fig.2, where data are given from the compilation [5]). The study of the forward angle reaction (1) by ITEP experiments [6] on  $^{16}O$  and  $^6Li$  in a kinematics which forbids real production of additional pion has demonstrated a relatively weak energy dependence of its rate and considerable excess over SSCX mechanism prediction [6] around  $T_0 = 1 GeV$ . So the conventional elastic SSCX picture of inclusive pion DCX has to be modified by an important new mechanism of IR at  $GeV$  energies.

Our goal is to elaborate recently suggested Gribov-Glauber approach to inclusive pion DCX reaction [4] on  $^{16}O$ . Below we present an updated analysis of some theoretical aspects of our model and clarify simplifying assumptions we have used. Then we estimate quantitatively upper and lower limits for inclusive pion DCX cross section in the energy region of  $T_0 = 1 GeV$  to 4  $GeV$  to be tested in future experiments. Our working scheme for the calculation of  $\pi \rightarrow 2\pi$  amplitude is the one pion exchange (OPE) model which we check by a comparison of theoretical cross section with experiment as well as distributions on two-pion effective mass for the process  $\pi^- p \rightarrow \pi^+ \pi^- n$ . We compare our results with predictions of other models and in particular of the meson exchange currents (MEC) model [7].

## 2 Gribov-Glauber picture of inclusive pion DCX

In this Section we shall discuss some aspects of the formalism for a calculation of the amplitude of the DCX process  $\pi^- pp \rightarrow \pi^+ nn$  (Fig.3). Following Gribov [8] it is convenient to introduce an integration over  $M_H^2$ , square of mass of the intermediate state in Fig.1. It is related to integration over Fermi motion of initial protons and momenta of final neutrons. These momenta are limited by experimental conditions. For example in the ITEP experiment on  $^6Li$  and  $^{16}O$  [6] the inclusive DCX reaction  $A(\pi^-, \pi^+)X$  was measured at kinetic energies  $T_0 = 0.6, 0.75$  and  $1.1 GeV$  ( $\langle \theta \rangle \approx 5^\circ$ ) with kinematical condition  $\Delta T = T_0 - T \leq m_\pi$  ( $T$  is the kinetic energy of the outgoing pion) in order to exclude additional pion production.

The kinematical region indicated above strongly limits momentum transfers  $t_{1(2)}$  to neutrons in the transitions  $\pi^- p \rightarrow Hn$  and  $Hp \rightarrow \pi^+ n$  (see Fig.3).  $M_H$  can be very large at high incident energy,  $E_0$ , and increases as  $M_H^2 \sim 2m_N E_0$ . The value of  $M_H^2$  varies also due to the Fermi motion. It is easy to obtain an estimate of this variation taking into account that at high energies,  $E_0 \gg m_N$ ,  $|t_{1(2)}^{min}| \approx (M_H^2 - m_\pi^2)^2 / 4E_0^2 \lesssim p_F^2 \lesssim 2m_N \Delta T_{1(2)}$  and  $(M_H^2)^{max} \approx 2E_0(2\Delta T_i m_N)^{1/2}$ . For energy  $E_0 \sim 1 \text{ GeV}$ ,  $(M_H^2)^{max}$  is equal to  $0.5 \text{ GeV}^2$ . As it was explained in Ref. [4], the integral over  $M_H^2$  can be written either over the real axis or (due to analyticity in  $M_H^2$ ) as a sum of the absorptive part and integral over semicircle at  $|M_H^2| \sim (M_H^2)^{max}$ . At high enough energies  $E_0$  the last contribution can be neglected if the corresponding amplitude decreases faster than  $1/M_H^2$  at large  $M_H^2$ . We gave arguments [4] that the amplitude of Fig.3 should satisfy this property. In this case the DCX amplitude is proportional to the discontinuity in  $M_H^2$  of the amplitude in Fig.3, and using unitarity we obtain the representation equivalent to the diagrams of Fig.1.

Contribution of a single particle intermediate state  $(\pi^0, \eta^0)$  or narrow resonance  $(\omega, \dots)$  to the DCX cross section can be written in the form

$$\frac{d\sigma_{DCX}^{IR}}{d\Omega} \propto \left( \int \int \frac{d^2\sigma_{\pi \rightarrow H}}{dt dM^2} dt dM^2 \right)^2, \quad H = \pi^0, \eta^0, \omega, \dots \quad (2)$$

Let us comment on contribution to DCX of different diagrams of Fig.1 that was taken in Ref.[4] additively. The diagram (b) gives a small correction to the Glauber elastic rescattering of Fig.1(a) due to the fact that  $\pi^- \rightarrow \eta$  amplitude is relatively small (see Fig.2) while the production of two pions is a very important competing mechanism, especially for  $T_0 \gtrsim 0.6 \text{ GeV}$ . As for diagrams (a) and (c), if  $\pi \rightarrow 2\pi$  amplitude is dominated by the pion exchange (see Fig.4), then their interference is absent. Really, the invariant form of the nucleon vertex in Fig.4 is  $\bar{u}\gamma_5 u$ , while the amplitude of the transition  $\pi^- p \rightarrow \pi^0 n$  is proportional to  $\bar{u}(A + B\hat{q})u$ , where  $q = p_{\pi^-} + p_{\pi^0}$ . So the interference term is  $\text{Tr}(\hat{p}_1 + m_N)\gamma_5(\hat{p}'_1 + m_N)(A + B\hat{q}) = 0$ .

Note that for the  $s$ -wave  $\pi\pi$  production which is a dominant inelastic process at energies  $E_0 \lesssim 1 \text{ GeV}$  the interference is absent by the same reason. For the  $s$  wave (and in general for all even waves) the same expression (2) is valid. However for realistic case of  $\pi\pi$  production, when both even and odd orbital momenta are important, the amplitude of  $\pi^- \rightarrow \pi^+$  transition (contrary to the diagonal  $\pi^- \rightarrow \pi^-$  transition) can not be written [4] in the form (2). This is especially clear in the  $\pi$  exchange (OPE) model (Fig.4) where DCX amplitude is expressed in terms of the  $\pi^- \pi^+ \rightarrow \pi^+ \pi^-$  amplitude (or backward

elastic  $\pi^-\pi^+$  scattering amplitude).

In this paper we shall use the OPE model in order to study the problems outlined above: is it possible to neglect the contribution of the large semicircle at energies  $\sim 1\text{ GeV}$  and what is the difference between integrals of forward and backward  $\pi^-\pi^+$  scattering amplitudes? In this way we shall find corrections  $\Gamma_H$  to simple expressions for DCX cross sections

$$\frac{d\sigma_{DCX}}{d\Omega} = \frac{d\sigma_{DCX}^{\pi^0}}{d\Omega} \left( 1 + \sum_H \Gamma_H \right) \quad (3)$$

where

$$\Gamma_{\pi^+\pi^-} = \left( \int dM \int_{t_{1\min}(M)}^{t_{1\max}^{\exp}} \frac{d^2\sigma_{\pi\rightarrow\pi^+\pi^-}(M, t_1)}{dM dt_1} dt_1 \bigg/ \int_0^{t_{1\max}^{\exp}} (d\sigma_{\pi^0}/dt_1) dt_1 \right)^2, \quad (4)$$

$$\Gamma_{\pi^0\pi^0} = \left( \sigma_{\pi\rightarrow\pi^0\pi^0}^{\text{tot}} / \sigma_{\pi\rightarrow\pi^+\pi^-}^{\text{tot}} \right)^2 \cdot \Gamma_{\pi^+\pi^-} \quad (5)$$

introduced in Ref.[4] and shall obtain lower and upper bounds for these cross sections at higher energies.

### 3 Inelastic rescatterings and comparison with ITEP experiment

In this Section we shall calculate the contribution of IR to DCX using Eqs.(3)-(5) and experimental data on particle production in reactions

$$\pi^- p \rightarrow H n, \quad H = \pi^0, \quad \pi^+\pi^-, \quad \pi^0\pi^0, \quad . . . \quad (6)$$

The quantities  $\Gamma_H$  in Eqs.(3)-(5) were determined using experimental data for the following hadronic states  $H$ :  $\pi^0$  [9],  $\pi^+\pi^-$  and  $\pi^0\pi^0$  [10]. While integrating over  $t$  and  $M^2$ , experimental constraints on  $\Delta T$  are taken into account (see details in [4]):  $|t_{1(2)}| \leq 2m_N(\Delta T^{\max}/2)$  [1].

In the Table 1 we show the updated summary of energy dependence for forward inclusive DCX reaction cross sections of  $\pi^-$  on  $^{16}\text{O}$  obtained in experiments at ITEP [6] and calculated via Eqs.(3)-(5). The first line in the Table 1 contains the values of  $d\sigma_{DCX}^{\pi^0}/d\Omega$  calculated [3,6] in the framework of the elastic SSCX mechanism without taking into account effect of the Fermi motion (FM) on magnitude of the  $\pi N$ -interaction energy in the nucleus. In the values  $d\tilde{\sigma}_{DCX}^{\pi^0}/d\Omega$  of the second line the FM effect <sup>2)</sup> is included. The resulting values

<sup>1)</sup> In principle it is necessary to integrate over  $t_1$  and  $t_2$ , but taking into consideration some uncertainty of the theoretical estimates as well as of the experimental information available we limited ourselves with this simple relation.

<sup>2)</sup> We thank L.Alvarez-Ruso and M.J.Vicente Vacas for preparing the version of the code [3] which takes into consideration the Fermi motion.

are  $d\sigma_{DCX}/d\Omega = d\tilde{\sigma}_{DCX}^{\pi^0}/d\Omega + (\Gamma_{\pi^+\pi^-} + \Gamma_{\pi^0\pi^0}) d\sigma_{DCX}^{\pi^0}/d\Omega$  are given at the fourth line. Due to a sharp change of DCX rate at energies of interest the FM effect gives smearing of the dip-bump structure, that in average leads in some increase of the values of DCX cross section. Note, that all values in the Table 1 correspond to the outgoing momentum spectra integrated over the region of  $\Delta T = 0$  to  $140 \text{ MeV}$ .

#### 4 Inclusive pion DCX in the energy range of 1 – 4 GeV

We see from the experimental data compilation of Fig.2 that the cross section values of the reaction (6) with  $H = \pi^+\pi^-$ ,

$$\pi^- p \rightarrow \pi^+ \pi^- n, \quad (6')$$

exceed ones with  $H \neq \pi^+\pi^-$  not only at 1 GeV but also at higher energies. So it is reasonable to assume that IR with two pion intermediate states will dominate inclusive pion DCX at least up to 4 GeV. In this case the diagram of Fig.4 can be used to obtain a quantitative estimate of DCX rate within the OPE model. Note here that, besides of the well-known good description of experiment for (6') reaction, the OPE model is very convenient to our goals because of its factorization feature. This permits to separate  $M^2$  and  $t$  dependences of the (6') reaction amplitude,  $A_{\pi \rightarrow 2\pi}(M^2, t)$ , and to take into account limitations on their values in the experiment [6].

We start from the following formula

$$\frac{d\sigma_{DCX}^{\pi\pi}}{d\Omega} \propto \left( \int_{4m_\pi^2}^{M^2(t_{max})} dM^2 \int_{t_{min}(M^2)}^{t_{max}} dt \text{Im} A_{\pi \rightarrow 2\pi}^{forward}(M^2, t) \right)^2 \quad (7)$$

equivalent to Eqs.(3)-(5). Then we use the OPE model [11] to calculate a difference between imaginary parts of forward and backward amplitudes and to estimate the real part of the amplitude.

In OPE model it is possible to express the amplitude of the process (6') in terms of the  $\pi\pi$  scattering amplitude,

$$A_{\pi \rightarrow 2\pi}(M^2, t) = \tilde{F}^2(t) A_{\pi\pi}(M^2) \quad (8)$$

where

$$\tilde{F}^2(t) = 2G^2 [|t|/(t - m_\pi^2)^2] \exp[2R^2(t - m_\pi^2)], \quad R^2 = 1.92 \text{ GeV}^{-2}, \quad (9)$$

$G$  is the  $\pi NN$ -coupling constant.

(a) *OPE model for DCX*

As it was shown in [11] the OPE model calculations are in a good agreement with the experimental data on the reaction (6') above  $2 \text{ GeV}$ . So for calculation of the cross section for this reaction we shall follow Ref.[11], namely:

$$\frac{d^2\sigma_{\pi\rightarrow 2\pi}}{dM^2 dt} = G^2 \frac{Q(M^2, m_\pi^2, m_\pi^2)M}{2^4\pi^2 Q^2(s, m_\pi^2, m_\pi^2)s} \tilde{F}^2(t) \sigma_{\pi\pi}^{tot}(M^2) \quad (10)$$

where  $G^2/4\pi = 14.6$ ,  $Q(s, m_1^2, m_2^2) = \sqrt{s^2 - 2s(m_1^2 + m_2^2) + (m_1^2 - m_2^2)^2}/2\sqrt{s}$ ,

$M$  is the mass of two-pion state,

$$\sigma_{\pi^+\pi^-}(M^2) = 2\pi \int |f_{\pi^+\pi^-}|^2 dz, \quad z = \cos\theta, \quad (11)$$

and the  $\pi\pi$  scattering amplitude is equal to

$$f_{\pi\pi}(M^2, z) = \frac{1}{Q(M^2)} \sum_l (2l+1) [1 + (-1)^{I+l}] f_l^I(M^2) P_l(z). \quad (12)$$

By virtue of the unitarity condition we have:

$$\text{Im} A_{\pi\pi}(M^2, z=1) = 2Q(M^2, m_\pi^2, m_\pi^2) M \sigma_{\pi\pi}^{tot}(M^2). \quad (13)$$

The partial-wave amplitudes  $f_l^I(M^2, z)$  for orbital angular momentum  $l$  and isospin  $I$  are expressed via the phase shifts,  $\delta_l^I$ , and elasticities,  $\eta_l^I$ :

$$f_l^I(M^2) = \frac{1}{2i} [\eta_l^I(M^2) e^{2i\delta_l^I(M^2)} - 1], \quad f_{\pi^+\pi^-} = \frac{1}{6} f^2 + \frac{1}{3} f^0 + \frac{1}{2} f^1. \quad (14)$$

It should be noted that the equation (7) takes into account both  $\pi^+\pi^-$  and  $\pi^0\pi^0$  intermediate states.

In the following we will use the complete set of amplitudes (phase shifts and elasticities) with  $l = 0, 2$  for  $I = 0, 2$  and with  $l = 1, 3$  for  $I = 1$  in the range of  $M$  up to  $\approx 1.8 \text{ GeV}$  from Ref.[12] where fixed- $t$  and fixed- $u$  analyticity in conjunction with energy independent phase-shift analysis gave the single solution. The following features of the model confirm that its predictions are reasonable.

(1) The  $M^2$  dependence of the total cross section of  $\pi^+\pi^-$  scattering calculated according to Eq.(11), (13), (14) is in a good agreement with the data from Ref.[13] (see Fig.5).

(2) The value of the parameter  $R^2 = 1.918 \text{ GeV}^{-2}$  that we use was obtained on the base of our analysis of the  $t$  dependence of the yield for the reaction (6')

averaged over the energy region from 2 to 3  $GeV$  taken from [11]. The total cross section of this reaction calculated via the integration of Eq.(10),

$$\sigma_{\pi^- p \rightarrow \pi^+ \pi^- n} = \int_{4m_\pi^2}^{M^2(t_{max})} dM^2 \int_{t_{min}(M^2)}^{t_{max}} dt \frac{d^2 \sigma_{\pi^- p \rightarrow \pi^+ \pi^- n}}{dM^2 dt} \quad (15)$$

(for  $t_{max} = t_{max}(s)$ ) is compared to experimental data (*full stars*) from Ref.[5] in Fig.6. It is seen that the model used (*full circles*) reproduces experimental energy behaviour of  $\sigma_{\pi^- p \rightarrow \pi^+ \pi^- n}$  only above  $\approx 2.5 GeV$ . Some underestimate of the absolute value of the cross section decreases as  $T_0$  increases.

In Fig.6 the cross section of the reaction (6'), obtained with constraints of  $t_{max} = t_{max}^{exp} = 0.135 (GeV/c)^2$  corresponding to the experimental limitation  $\Delta T \leq 140 MeV$ , is also presented. The experimental values (*crosses* and *empty star*) were calculated from the data of Ref.[10a] on  $M^2$  and angular cross-section dependencies of the reaction (6') (*crosses*) and taken from Ref.[14] for the interval  $1.5 \leq t/m_\pi^2 \leq 8$  (*empty star*). The OPE model used (*triangles* in Fig.6) agrees with experiment starting already from 1  $GeV$ . Note that below  $T_0 = 1 GeV$  the OPE model predictions strongly deviate from experimental data. This is probably related to a substantial role of  $s$ -channel resonance production in this region.

(3) The experimental distributions on the two-pion mass ( $M$  or  $M^2$ ) for incident momentum values of 1.343 [10], 1.59 [14], 2.26 [15], and 4  $GeV/c$  [16] are compared with the calculated ones (see Figs. 7-10). It is seen from Fig.7 that the model predicts too small cross section in the low  $M^2$  region at the lowest energy. On the other hand, at higher energies the OPE model reproduces experiment rather well (including  $\rho$  and  $f_2(1270)$  resonances as it is seen in Figs. 9, 10). For our purpose it is essential to have a good description of experiment in  $t$  interval close to  $t \leq 0.135 (GeV/c)^2$ . It follows from Fig.8 that for the region of  $1.5 \leq t/m_\pi^2 \leq 8$  an agreement with experiment is better than for the total cross section of (6').

Thus we conclude that it is reasonable to use the OPE model for calculation of the high-energy DCX cross section.

#### b) Tests of the assumptions

Now it is interesting to use the OPE model calculations for checking of the simplifying assumptions of our approach to DCX formulated in Ref.[4] and discussed above.

The real and imaginary parts of forward ( $z = 1$ ) and backward ( $z = -1$ ) invariant amplitude,  $A_{\pi^+ \pi^-}(M^2, z)$ , were calculated using Eqs.(12) – (14). As

can be seen from Fig.11,  $\text{Re}A_{\pi^+\pi^-}(M^2, z = -1)$  oscillates but it is not small compared to  $\text{Im}A_{\pi^+\pi^-}(M^2, z = -1)$  so its contribution should be taken into account at energies  $\sim 1 \text{ GeV}$ . This means that an integral over  $\text{Re}A_{\pi^+\pi^-}(M^2, z = -1)$  can not be neglected in this energy range and thus the same is true for integral over the large semicircle. The backward parts of the amplitude appeared to be rather different from the forward ones within various intervals of  $M^2$ . The actual ranges of  $M^2$  for a set of initial energies for experimental data available on the reaction (6') are given in the Table 2.

In the Fig.12 we present the energy dependence of the cross section  $d\sigma_{DCX}^{\pi\pi}/d\Omega$  calculated according Eq.(7) at  $M_{max}^2|_{140}$  for the following cases:

- (1)  $\text{Im}A_{\pi \rightarrow 2\pi}^{forward}$  is obtained through the Eq.(8) for the forward ( $z = 1$ ) amplitudes;
- (2)  $\text{Im}A_{\pi \rightarrow 2\pi}^{forward}$  is replaced by  $\text{Im}A_{\pi \rightarrow 2\pi}^{backward}$  which is obtained according to Eq.(8) for the imaginary part of the backward ( $z = -1$ )  $\pi\pi$  amplitude;
- (3) Same as in (2), but for  $\text{Re}A_{\pi \rightarrow 2\pi}^{backward}$ ;
- (4) both imaginary and real parts of the backward amplitude are taken into account.

The above analysis shows that for  $\pi^+\pi^-$ -scattering amplitudes there are substantial differences between integrals of forward and backward scattering amplitudes and they can be neglected only at rather low energies, where  $s$ -wave production dominates. We think however that OPE model overestimates this difference, especially for  $T_0 \lesssim 1 \text{ GeV}$ , as it predicts too low  $s$ -wave production at these energies (see Fig.7). So the OPE-result for DCX can be considered as a lower bound for this cross section.

## 5 Results

Let us now calculate the cross section for the reaction

$$\pi^- + {}^{16}\text{O} \rightarrow \pi^+ + X \quad (16)$$

in the kinematical range  $0 \leq \Delta T \leq 140 \text{ MeV}$  of the experiment [6] as a sum of the cross sections with  $\pi^0$  and  $2\pi$  in intermediate states (see Eq.(3) ),

$$\langle \frac{d\sigma_{DCX}}{d\Omega} \rangle_{140} = \langle \frac{d\tilde{\sigma}_{DCX}^{\pi^0}}{d\Omega} \rangle_{140} + \langle \frac{d\sigma_{DCX}^{\pi\pi}}{d\Omega} \rangle_{140}. \quad (17)$$

Here  $\langle d\tilde{\sigma}_{DCX}^{\pi^0}/d\Omega \rangle_{140}$  is the cross section of the reaction (16) within the SSCX mechanism (FM effect is taken into account) which is shown in Fig.13 (see *dashed* curve).  $\langle d\sigma_{DCX}^{\pi\pi}/d\Omega \rangle_{140}$  is the contribution of the intermediate  $\pi\pi$  state



for the given kinematical range of  $\Delta T$ . For  $\text{Im}A_{\pi \rightarrow 2\pi}^{\text{forward}}$  according to Eqs.(3)-(5) and normalizing at  $T_o = 0.6 \text{ GeV}$  we obtain the *dotted curve* in Fig.13. The solid curve corresponds to an account of the full backward scattering amplitude. It can be considered as a lower bound for the DCX cross section, while the dotted curve can be considered as an upper bound for the cross section. Experimental point at  $1.1 \text{ GeV}$  is close to this bound. This is related in our opinion to an underestimate of the  $s$ -wave contribution in the OPE model at these energies noted above. So at higher  $T_0$  we expect future DCX measurements to be closer to the solid curve. Note, that both curves at  $T_o < 1 \text{ GeV}$ , where OPE model strongly deviates from experimental data (see Fig.6), are calculated using not theoretical but experimental values (see the first two *crosses* in Fig.6).

The contribution from three-pion intermediate state to Eq.(17) estimated using the cross section of  $\pi^- p \rightarrow \omega n$  appeared to be not more than 10% even at the highest energy considered.

## 6 Comparison with other approaches

Let us discuss a relation between inelastic rescatterings considered in this paper, and other approaches which have been proposed for the DCX process.

Relation of the present approach to a model of meson exchanged currents (MEC) [18] has been discussed in Ref.[4]. The main difference is that in the OPE model we treat the  $\pi^- \pi^+$ -scattering amplitude as a function of  $M^2$  and integrate over this variable while in the MEC model the  $\pi^- \pi^+$ -amplitude is approximated as a point-like interaction taken at the threshold ( $M = 2m_\pi$ ). Due to soft pion theorems this amplitude is small and thus leads to small modifications of SSCX predictions [7]. We take into account in the OPE model both real and imaginary parts of  $\pi^- \pi^+$  amplitude in the regions of  $M^2$  where they are not small, so it is not surprising that our results for DCX cross sections are substantially higher than SSCX predictions (even for a solid curve in Fig. 13).

Another possible mechanism of DCX [19] is a production of an intermediate  $\Delta$  isobar on one proton of a nucleus,  $\pi^- p \rightarrow \pi^+ \Delta^-$ , with its absorption [20] on a second proton,  $\Delta^- p \rightarrow nn$ . A characteristic feature of this mechanism is a fast decrease of DCX cross section at  $T_0 > 1 \text{ GeV}$  due to energy dependence of the  $\sigma(\pi^- p \rightarrow \pi^+ \Delta^-)$  as is shown in Fig.2 by the curve.

Our study shows that at least up to energies  $\sim 4 \text{ GeV}$  the region of  $M_H^2 \sim M_{max}^2$  is very essential in integrals over  $M_H^2$ , and integrals of both imaginary and real parts of amplitudes are important. This means that average distances,  $d$ ,

between participating nucleons are relatively small:  $d \sim (2m_N \Delta T)^{-1/2}$ . These nucleons are closely correlated and can be even considered as a 6-quark system (as, for example, in Ref.[21]).

## 7 Experimental outlook and conclusions

We have extended the conventional Glauber mechanism for DCX process with an account of inelastic rescatterings. In this paper we investigated the problems which arise due to a non-diagonal nature of the process using the OPE model. This model gives a reasonable description of the reaction  $\pi^- p \rightarrow \pi^- \pi^+ n$  at energies above 2  $GeV$ . So we think that our predictions for DCX process based on this model, which are substantially higher than SSCX results, are reliable in this energy region. DCX is not yet studied experimentally at energies above  $T_0 = 1.1 GeV$ . If strong deviations from our predictions will be found it will have important implications: either other mechanisms (e.g. those mentioned in the previous Section) are important or the phase-shift analysis of  $\pi\pi$  scattering [12], which we have used, is not reliable in the large-mass region. An interesting information on these problems can be obtained by varying experimental interval of  $\Delta T$ . Note that for small  $\Delta T$  (and in particular in the exclusive limit) an integration region in  $M^2$  is small, and results should be closer to SSCX predictions.

Thus experimental study of the energy dependence of DCX in the region of  $T_0 = 1 \div 5 GeV$  can give an important information on dynamics of this process. Cross section in this region according to our estimate is not too small, and experiments seems feasible. However, at higher energies the possibility to measure the cross section in the region of  $\Delta T = 0 \div 140 MeV$  will be limited by the energy resolution of the detector.

In conclusion, it is important to stress once more that the investigation of the pion DCX reactions in the intermediate energy region can provide a test on a validity of the Glauber–Gribov approach in the case when effects of inelastic rescatterings are large. Another class of processes where such inelastic contributions are very important is heavy ions interactions at very high energies. It is known (see, for example, [22]) that these contributions strongly modify a usual Glauber picture and an equilibration in the system can appear only as a result of such rescatterings effects.

## Acknowledgments

A.P.K. thanks I.S. and I.I.Tsukerman for permanent support. This work was supported in part by RFBR Grant No. 98-02-17179.

## References

- [1] H.Clement, Progr. Part. Nucl. Phys. **29**, 175 (1992);  
M.B.Johnson, and C.L.Morris, Annual Rev. Nucl. Part. Sci. **43**, 165 (1993).
- [2] E.Oset, and D.Strottman, Phys. Rev. Lett. **70**, 146 (1993).
- [3] M.J.Vicente Vacas, M.Kh.Khankhasayev, and S.G.Mashnik, Preprint FTUV/94-73 University of Valencia 1994.
- [4] A.B.Kaidalov and A.P.Krutenkova, Yad. Phys. **60**, 1334 (1997) (Phys. At. Nucl., **60**, 1206 (1997)).
- [5] V. Flaminio et al., CERN-HERA 83-01, 30 August 1983, Compilation of cross-sections: I:  $\pi^+$  and  $\pi^-$  induced reactions.
- [6] (a) B.M.Abramov et al., Yad. Fiz. **59**, 399 (1996) (English translation: Phys. Atomic Nucl. **59**, 376 (1996));  
(b) B.M.Abramov et al., Few-Body Systems Suppl. **9**, 237 (1995).
- [7] L.Alvarez-Ruso, and M.J.Vicente Vacas, J. Phys. G: Nucl. Part. Phys. **22**, L45 (1996).
- [8] V.N.Gribov, ZhETF **56**, 892 (1969) (English translation: Sov. Phys. JETP **29**, 483 (1969)).
- [9] R.A.Arndt et al., Phys. Rev. C **52**, 2120 (1995);  
A.D.Brown et al., Nucl. Phys. B **153**, 89 (1979)
- [10] (a) A.D.Brody et al., Phys. Rev. D **4**, 2693 (1971);  
(b) D.M.Manley et al., Phys. Rev. D **30**, 904 (1984)
- [11] K.G.Boreskov, A.B.Kaidalov, and L.A.Ponomarev, Yad. Fiz. **17**, 1285 (1973).
- [12] J.L. Basdevant, C.D. Froggatt and J.L. Petersen, Nucl. Phys. **B72**, 413 (1974);  
C.D. Froggatt and J.L. Petersen, Nucl. Phys. **B129**, 89 (1977).
- [13] B.Y. Oh, A.F. Garfinkel, R. Morse et al., Phys. Rev. **D1**, 2494 (1970).
- [14] J. Alitty et al. Nuovo Cim. **29**, 515 (1963).
- [15] B.G. Reinolds et al. Phys. Rev. **184**, 1424 (1969).
- [16] L. Bondar et al. Nuovo Cim. **31**, 729 (1964).
- [17] S.A.Wood et al., Phys. Rev. C **46**, 1903 (1992).
- [18] J.-F.Germond, and C.Wilkin, Lett. Nuovo Cim. **13**, 605 (1975);  
M.R.Robilotta, and C.Wilkin, J. Phys. G: Nucl. Phys. **4**, L115 (1978).
- [19] C.L.Morris et al., Acta Phys. Polon. **24**, 1659 (1993)
- [20] O.D. Dalkarov and I.S. Shapiro, Phys.Lett. **B26**, 708 (1968).
- [21] G.A.Miller, Phys. Rev. **C35**, 377 (1987).
- [22] A.B.Kaidalov, Nucl. Phys. **A525**, 39c (1991).

$T_0, \text{ GeV}$	0.6	0.75	1.12
$d\sigma_{DCX}^{\pi^0}/d\Omega, \mu b/sr$ [8]	125.0	10.4	3.1
$d\tilde{\sigma}_{DCX}^{\pi^0}/d\Omega, \mu b/sr$	139.3	25.4	4.7
$\Gamma_{\pi^+\pi^-} + \Gamma_{\pi^0\pi^0}$	0.11	1.75	11.3
$d\sigma_{DCX}/d\Omega, \mu b/sr$	153.1	43.6	39.7
$d\sigma_{DCX}^{\text{exp}}/d\Omega, \mu b/sr$ [6]	$59.6 \pm 7.4$	$43.3 \pm 5.5$	$26.6 \pm 8.9$

Table 1.

$T_0, \text{ GeV}$	$M_{max}^2(s)$	$M_{max}^2(s) _{140}$
0.61	0.36	0.36
0.88	0.57	0.51
1.02	0.69	0.60
1.20	0.84	0.69
1.45	1.08	0.84
1.76	1.74	1.02
2.12	2.02	1.26
2.86	2.5	1.68
3.86	3.2	2.2

Table 2.

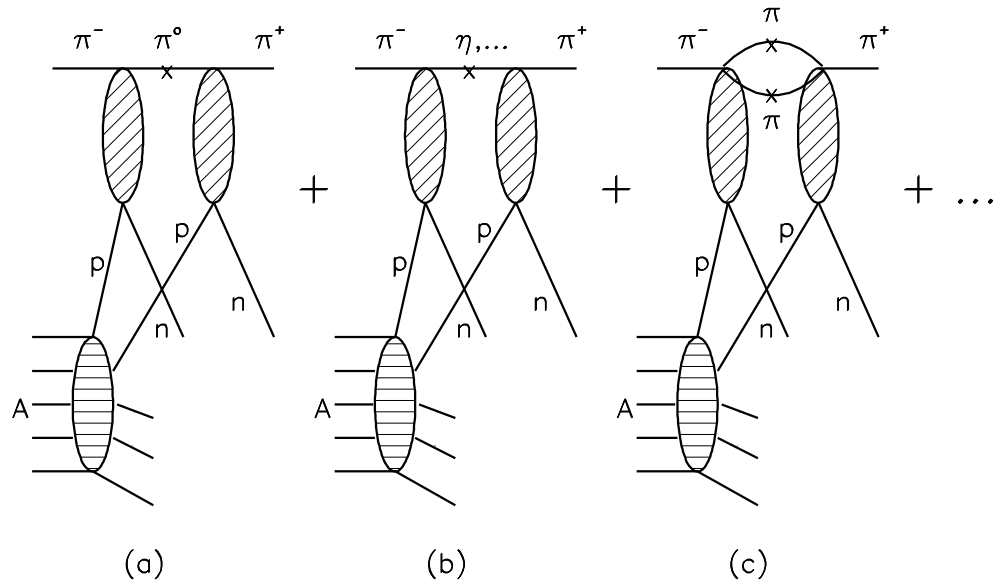


Figure 1: Diagrams contributing to pion double charge exchange on nuclei: (a) sequential single charge exchanges (SSCX), i.e. standard mechanism (elastic rescattering), (b) quasielastic rescatterings, (c) inelastic rescatterings.

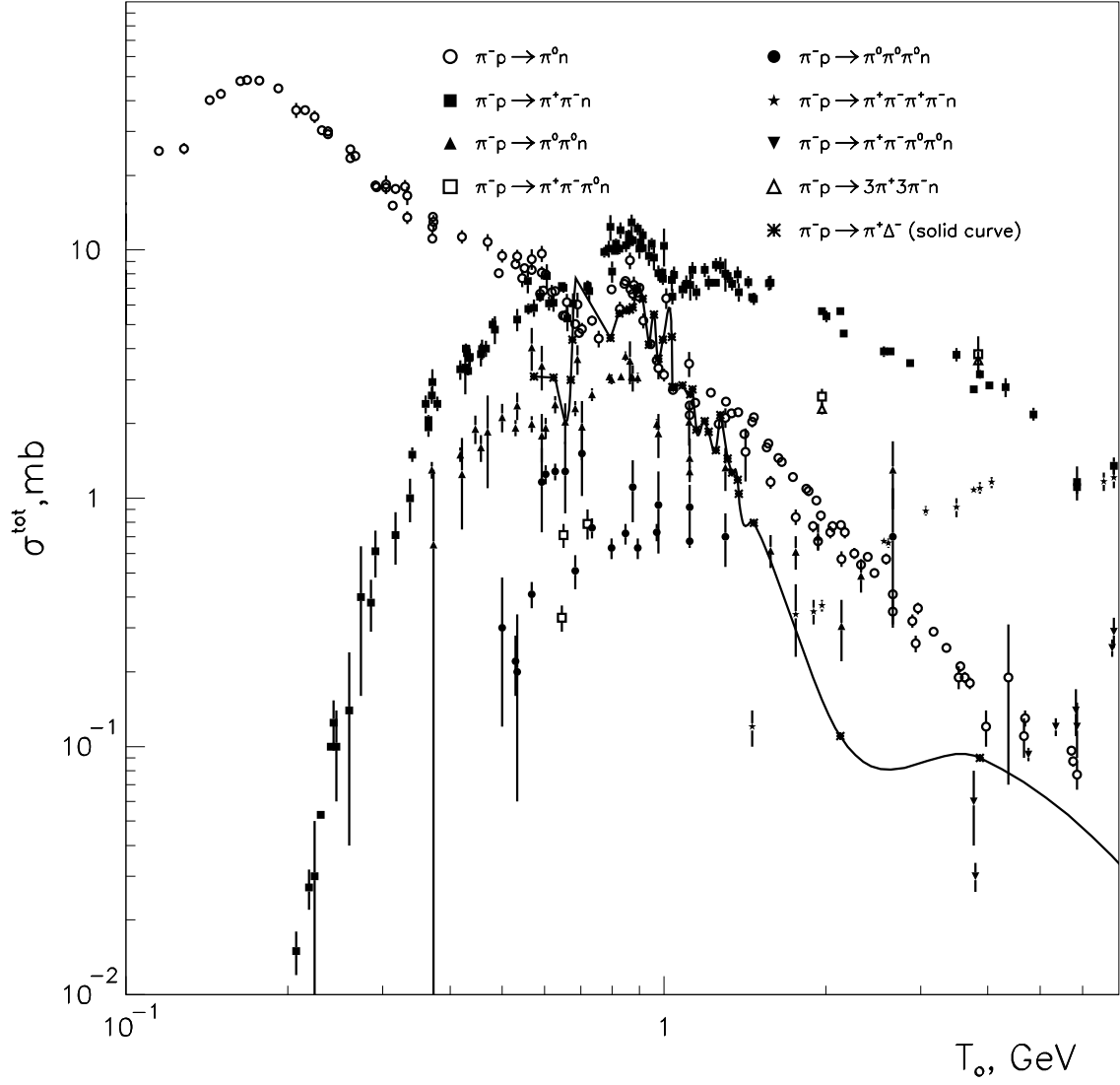


Figure 2: Experimental total cross section of the reaction  $\pi^- p \rightarrow H n$  and  $\pi^- p \rightarrow \pi^+ \Delta^-$  (see compilation [5]).

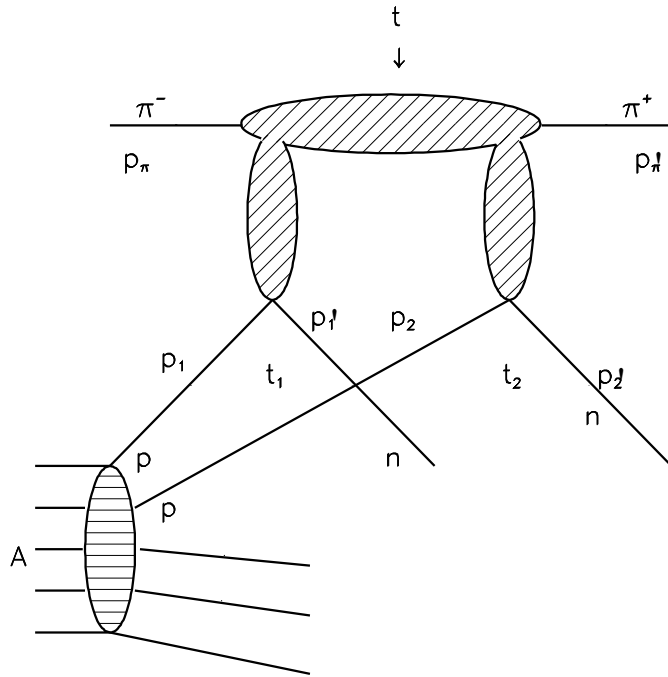
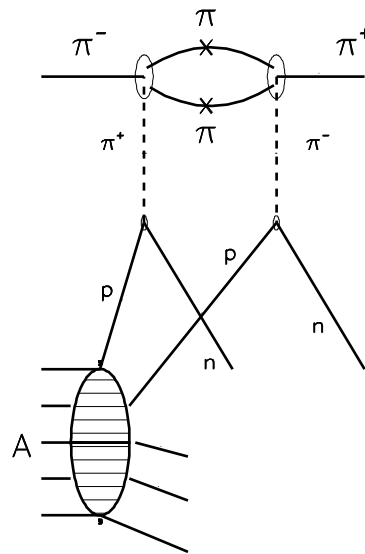


Figure 3: Pion double charge exchange on nucleus (the most general diagram).





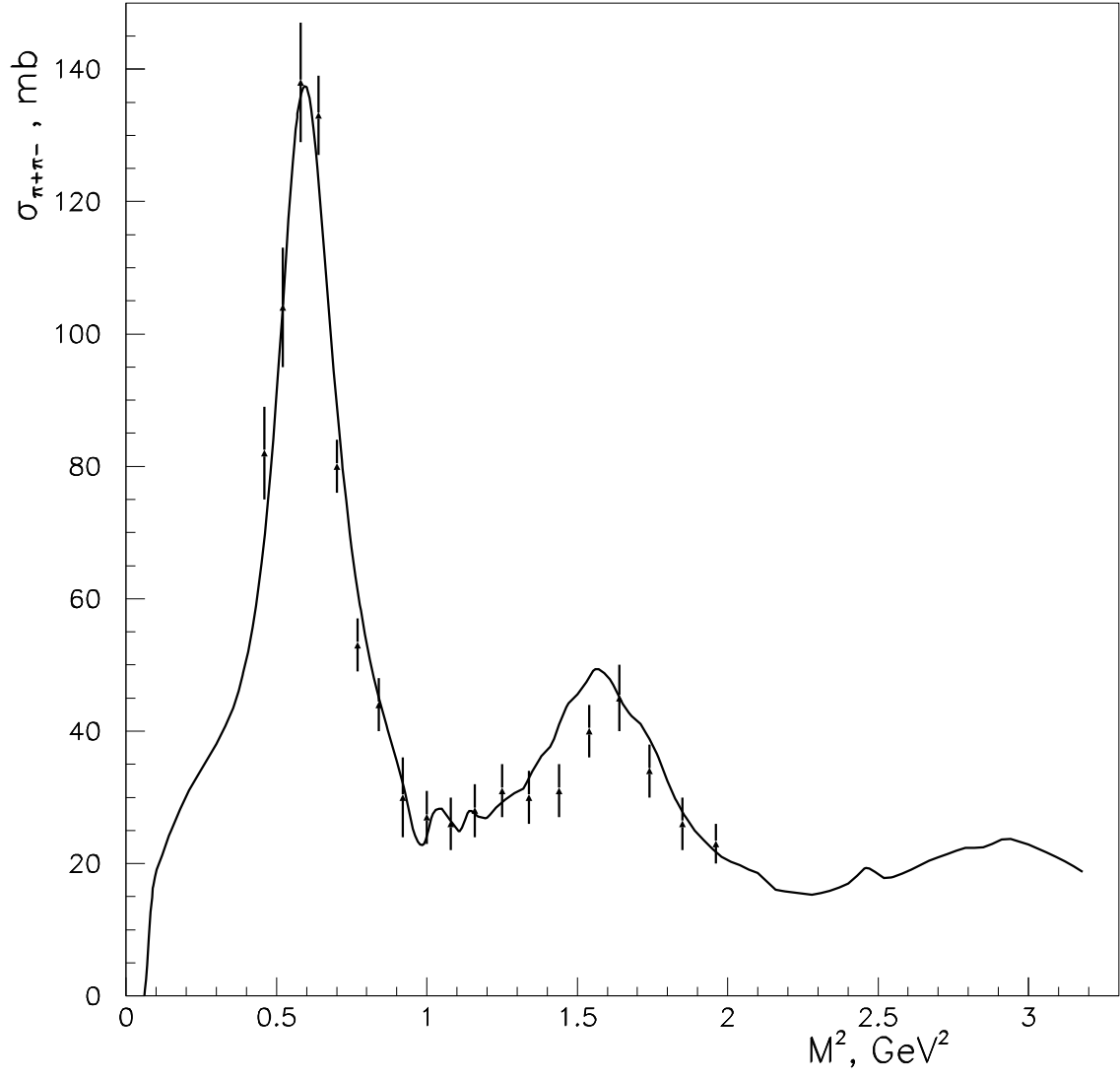


Figure 5: Total cross section of the reaction  $\pi^+\pi^- \rightarrow \pi^+\pi^-$  from [13]; the solid curve is our calculation.

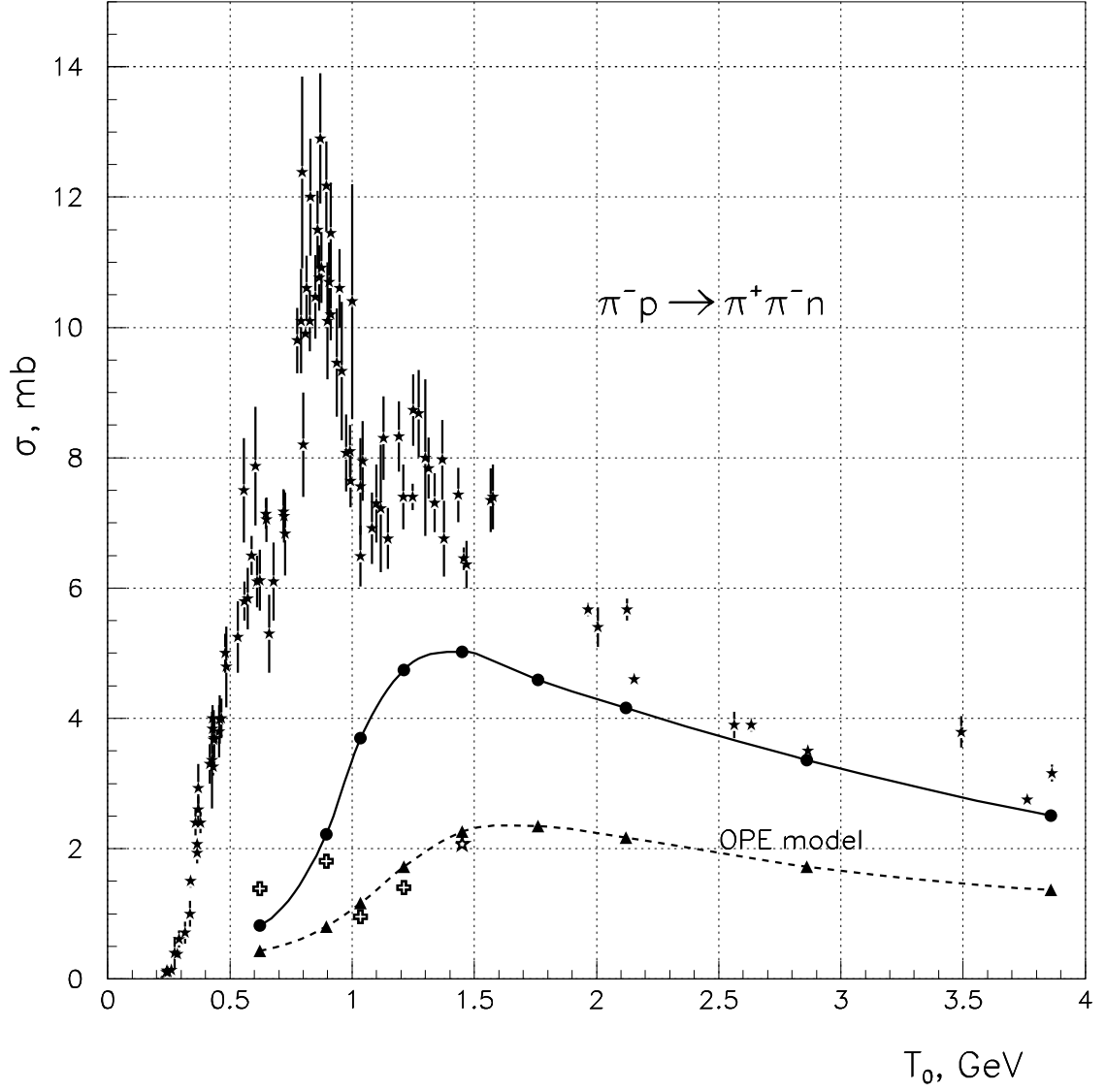


Figure 6: Total cross section of the reaction  $\pi^-p \rightarrow \pi^+\pi^-n$ . Stars and circles are experimental [5] and OPE cross sections, crosses and triangles are their corresponding truncated values for the  $\Delta T \leq 140$  MeV; empty star is for limited  $t$  (see text).

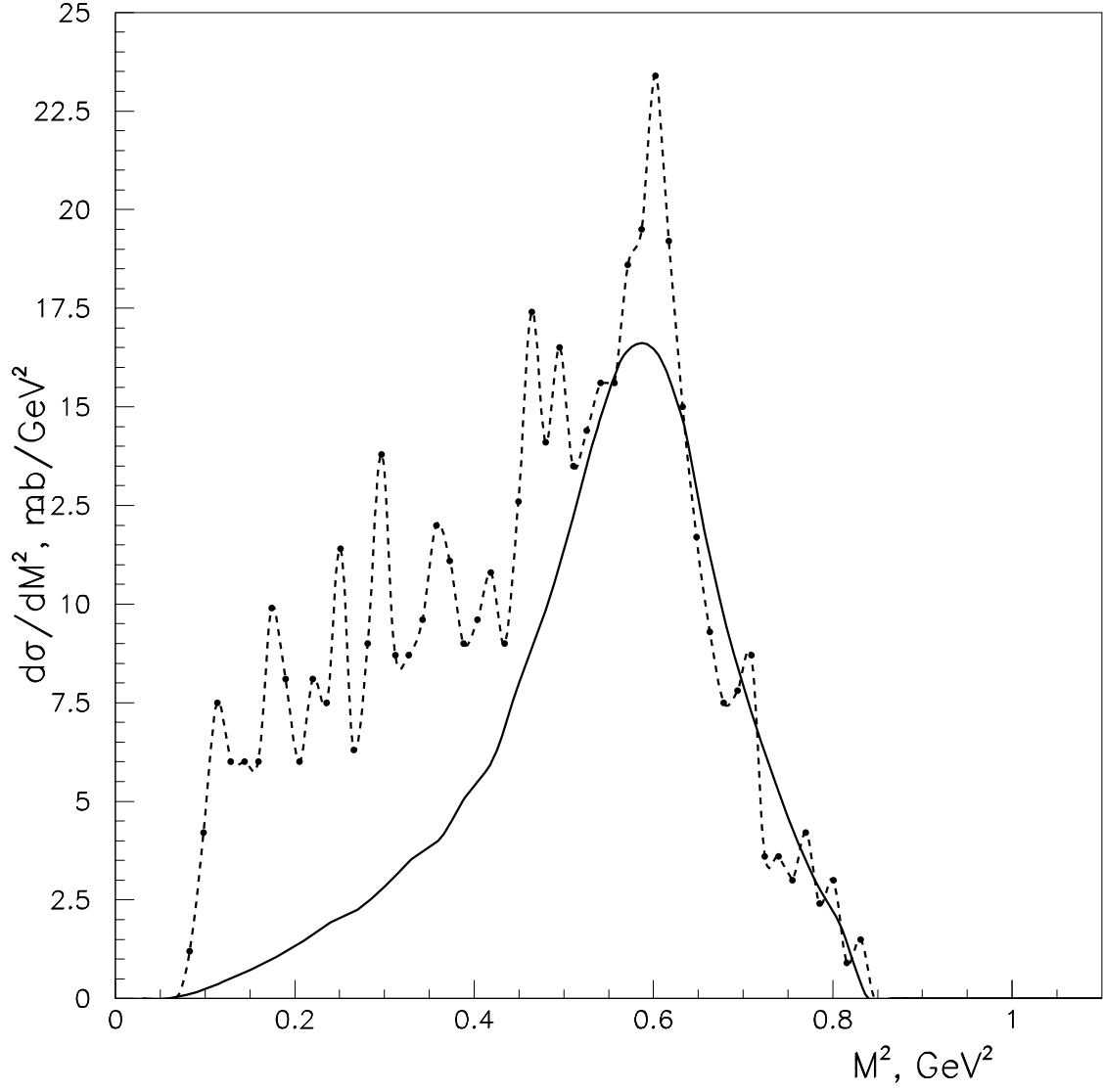


Figure 7: Mass-squared distribution of  $\pi^+\pi^-$  system in the reaction  $\pi^-p \rightarrow \pi^+\pi^-n$  [10a] at  $p = 1.343 \text{ GeV}/c$ . The solid curve is our calculation.

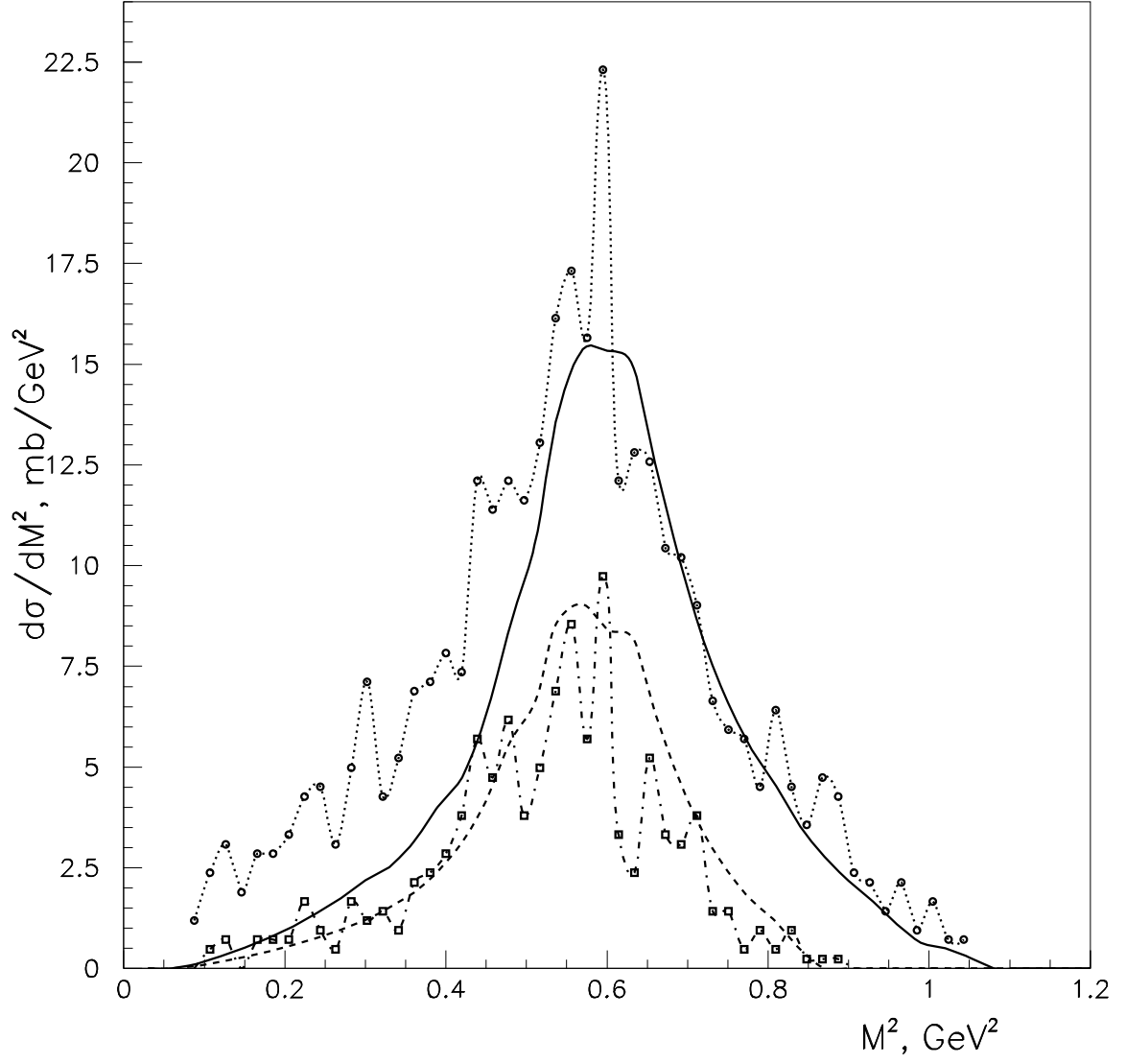


Figure 8: Mass-squared distribution of  $\pi^+\pi^-$  system in the reaction  $\pi^-p \rightarrow \pi^+\pi^-n$  [14] at  $p = 1.59 \text{ GeV}/c$ , open circles correspond to full range of  $t$ , open squares are for limited  $t$  (see text), the solid and dashed curves are our calculation.

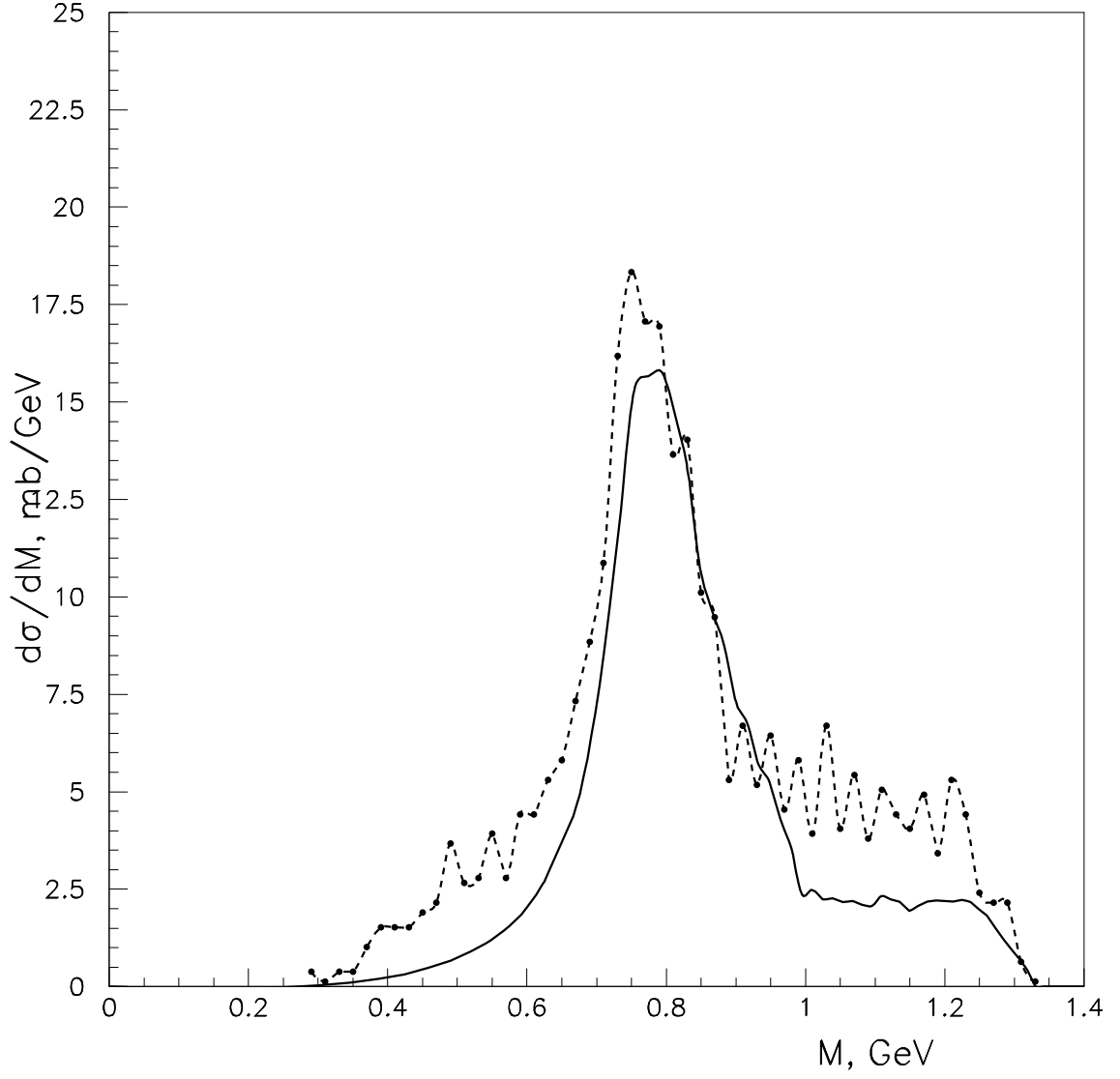


Figure 9: Mass distribution of  $\pi^+\pi^-$  system in the reaction  $\pi^-p \rightarrow \pi^+\pi^-n$  [15] at  $p = 2.26 \text{ GeV}/c$ . The solid curve is our calculation.

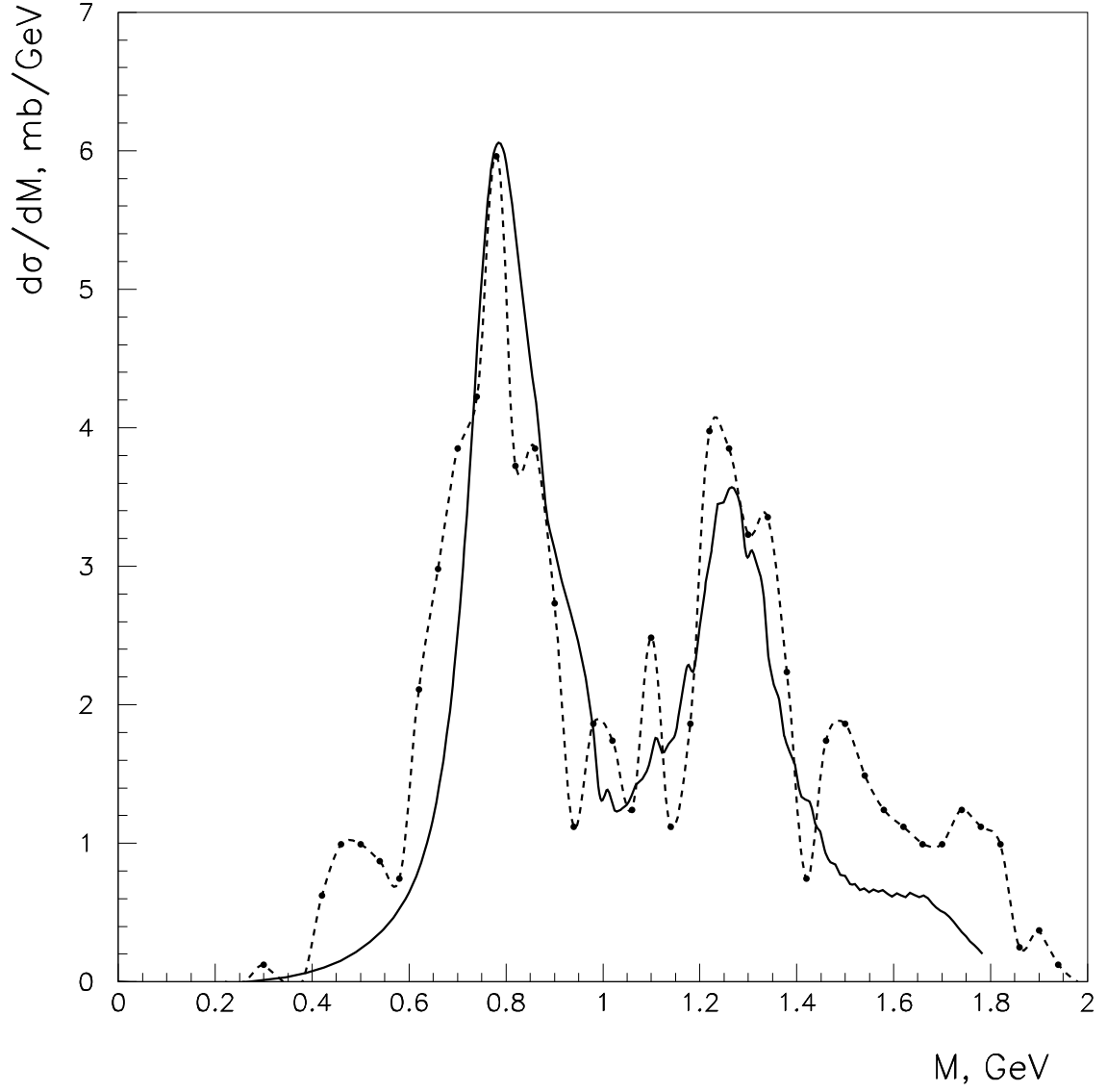


Figure 10: Mass distribution of  $\pi^+\pi^-$  system in the reaction  $\pi^-p \rightarrow \pi^+\pi^-n$  [16] at  $p = 4 \text{ GeV}/c$ . The solid curve is our calculation.

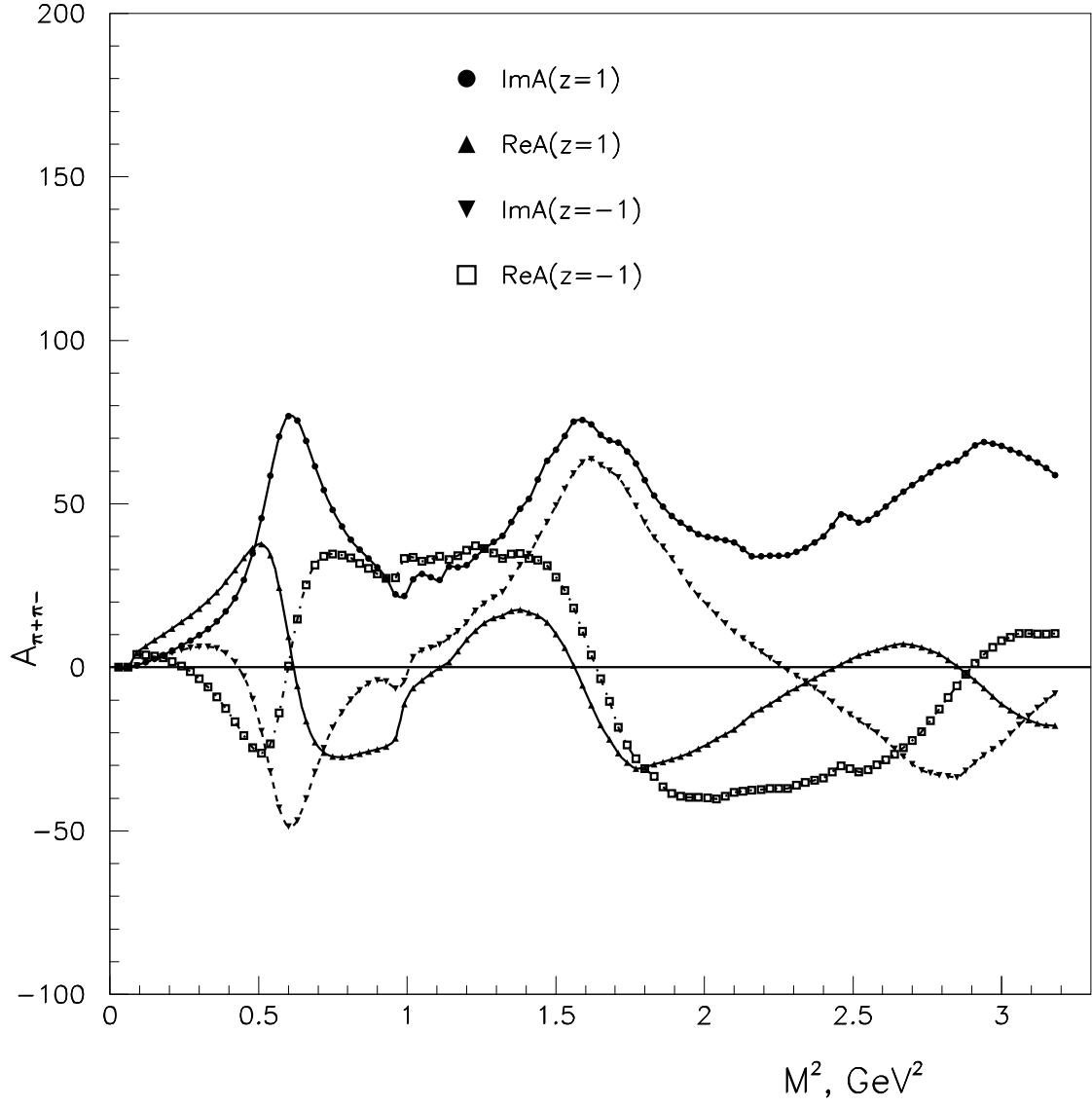


Figure 11: Invariant  $\pi^+\pi^-$  scattering amplitudes within OPE model.

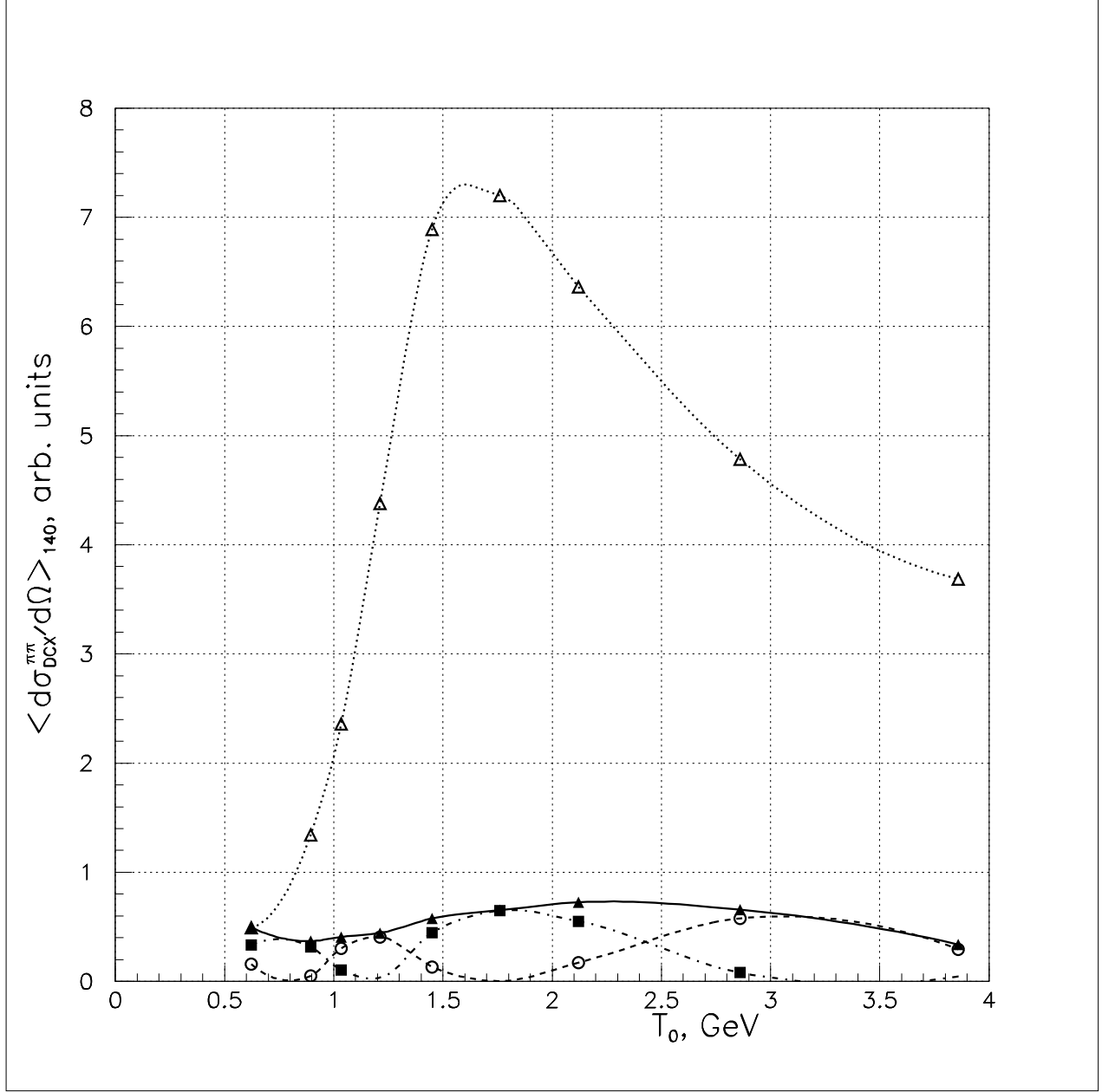


Figure 12:  $\langle d\sigma^{\pi\pi}/d\Omega \rangle_{140}$  calculated using  $\text{Im}A(0)$  in Eq.(7) (empty triangles),  $\text{Im}A(z = -1)$  (full triangles),  $\text{Re}A(z = -1)$  (empty circles), and both  $\text{Re}A(z = -1)$  and  $\text{Im}(z = -1)$  (full squares).



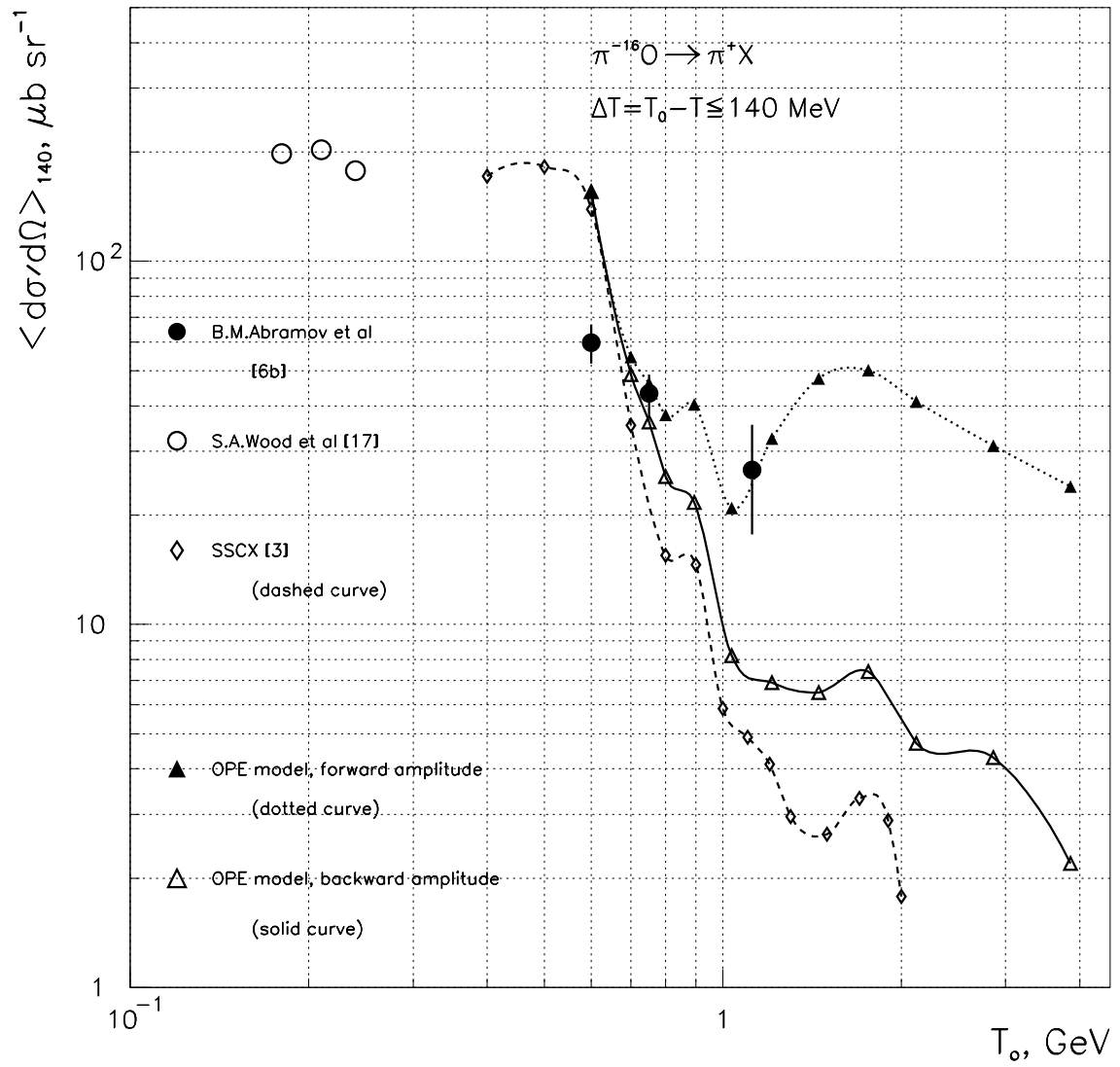


Figure 13:  $\sigma_{DCX}$  integrated over  $\Delta T$  range from 0 to 140 GeV.